Mistargeted MRPΔF728 mutant is rescued by intracellular GSH

Frédéric Buyse, Michel Vandenbranden, Jean-Marie Ruysschaert*

Structure et Fonction des Membranes Biologiques (S.F.M.B.), Centre de Biologie Structurale et de Bioinformatique, Université Libre de Bruxelles, CP 206/2, Bd. du Triomphe, B-1050 Brussels, Belgium

Received 3 August 2004; revised 22 October 2004; accepted 25 October 2004

Available online 16 November 2004

Edited by Gerrit van Meer

Abstract The most common cystic fibrosis-causing mutation is the deletion of the widely conserved phenylalanine 508 (ΔF508) of CFTR. The mutant is unable to fold correctly and to transit to the plasma membrane. MRP1 belongs to the same subfamily of ABC proteins as CFTR and confers resistance to a wide range of chemotherapeutic drugs. By analogy, phenylalanine 728 was deleted in MRP1. Our results shown that MRPΔF728 is correctly targeted to the plasma membrane, actively transports doxorubicin (DOX) and vincristine (VCR) and shares a structure identical to MRP1. Intracellular GSH depletion however results in a mistargeted mutant that is retained into the cytoplasm, while in the same conditions wild-type MRP1 is correctly routed to the plasma membrane. The GSH-protein complex could adopt a stable conformation protected against proteolytic degradation and correctly targeted to the plasma membrane.

Keywords: ABC; MRP1; MRPΔF728; Infrared spectroscopy; Membrane targeting; Fluorescence microscopy

1. Introduction

Cystic fibrosis transmembrane conductance regulator (CFTR) is a membrane chloride channel located in the apical membrane of many chloride secreting and reabsorbing epithelial cells [1]. This protein belongs to the ABCC subfamily of the ATP-binding cassette transporter superfamily ABC. It is composed of two nucleotide-binding domains (NBD1 and NBD2) and two transmembrane domains (TMD1 and TMD2), each spanning the membrane six times. CFTR also contains a large cytosolic regulatory (R) domain between NBD1 and TMD2, which is the site of regulatory phosphorylation [2]. A mutation (ΔF508) located in the center of the NBD1 domain of CFTR (42 amino acids after the Walker A site and 60 before the Walker B site, see Fig. 1) is mainly responsible for a disease called cystic fibrosis (CF) [1]. This mutation causes a misfolding of the protein that is not targeted correctly to the apical membrane but is retained in the endoplasmic reticulum (ER) in an inactive form that is rapidly degraded [4–6].

Susan Cole and Roger Deeley discovered multidrug resistance-associated Protein 1 (MRP1) in 1992 [3]. This membrane protein belongs to the same ABCC subfamily of membrane transporters as CFTR [46]. It confers resistance to a wide range of chemotherapeutic drugs including anthracyclines, *vinca* alkaloids and epipodophyllotoxins by rejecting them out of the cells [7–9]. This transport mechanism requires ATP binding and hydrolysis and for these drugs, the presence of GSH [10–13]. MRP1 is an ATP-dependent transporter of anionic compounds such as LTC_4, methotrexate or glutathione-, sulfate- and glucoronide-conjugated organic anions. The transport of such compounds is GSH-independent [14–16]. GSH itself also is a MRP1 substrate. Drug binding to MRP1 occurs through interactions with transmembrane domains [17–19] while NBDs are responsible for ATP binding and hydrolysis and for coupling energy release to substrate transport.

As CFTR, MRP1 is constituted of a typical ABC structure core containing two nucleotide-binding domains (NBD1 and NBD2) and two transmembrane domains (TMD1 and TMD2), each spanning the membrane six times. MRP1 contains an additional membrane domain spanning the membrane five times (TMD0) and linked to the N-terminal TMD1 domain by a cytoplasmic loop L0 [1,20,21]. The role of this additional domain is for the moment not understood.

In this study, we analyzed the effect of the deletion of phenylalanine at position F728 in MRP1. This residue is located exactly at the same position in MRP1 as F508 in CFTR with respect to the Walker sites, in a sequence conserved among the MRP subfamily (Fig. 1). Unlike CFTRΔF508, MRPΔF728 is correctly targeted to the plasma membrane and transports MRP1 substrates. However, intracellular GSH depletion leads to an intracellular localization of the mutant.

2. Materials and methods

2.1. Materials

Antiproteases (Complete EDTA-free) were purchased from Roche Diagnostics; Talon cobalt affinity resin from Clontech; QuikChange XL™ site-directed mutagenesis kit from Stratagene; primary mouse monoclonal antibody MRPm6 from Chemicon International; ECL Plus Western Blotting detection reagent from Amersham Biosciences; propidium iodide and Alexa Fluor 488 from Molecular Probes; MTT reagent and BSO from Sigma; MicroSpin G-25 column from Amersham Pharmacia Biotech. Plasmid pRC/CMV-MRP1 (wild-type)

*Corresponding author. Fax: +32 2 6505382.
E-mail address: jzmruyss@ulb.ac.be (J.-M. Ruysschaert).

Abbreviations: ABC, ATP binding cassette; ATP, adenosine-5′-triphosphate; ATR, attenuated total reflection; BSO, DL-buthionine-[S,R]-sulfoximine; CFTR, cystic fibrosis conductance regulator; DMSO, dimethyl sulfoxide; DOX, doxorubicin; FTIR, Fourier transform infrared spectroscopy; GSH, glutathione; H/D, hydrogen/deuterium; HEK, human embryonic kidney; LTC_4, leukotrienes C_4; MDR, multidrug resistance; MTT, 3-(4,5-dimethylthiazol-2-yl)-2,5-diphenyl tetrazolium bromide; MRP, multidrug resistance protein; NBD, nucleotide binding domain; PCR, polymerase chain reaction; Pgp, P-glycoprotein; TMD, transmembrane domain; VCR, vincristine

0014-5793/$22.00 © 2004 Published by Elsevier B.V. on behalf of the Federation of European Biochemical Societies.
doi:10.1016/j.febslet.2004.10.089

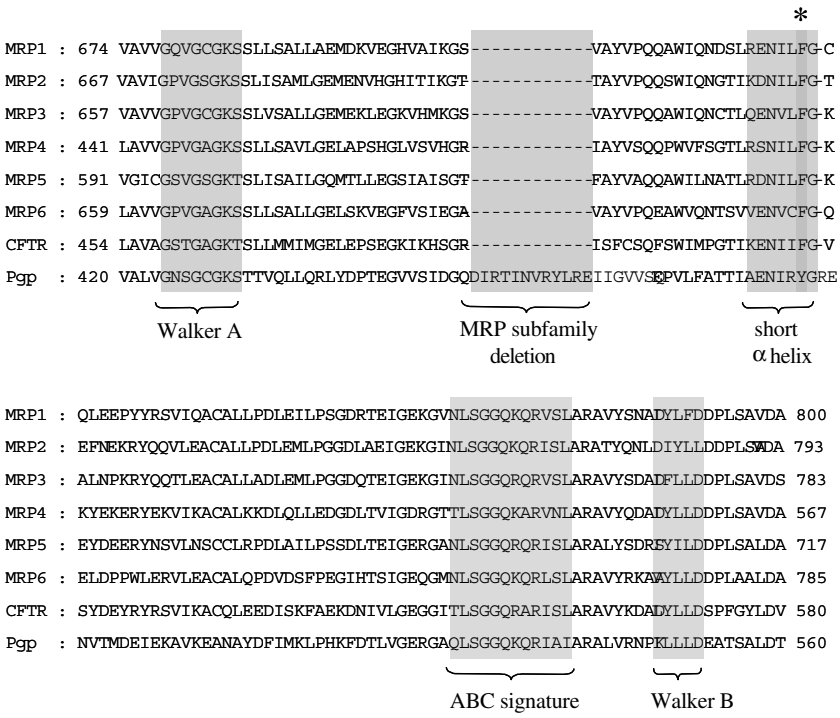

Fig. 1. Alignment of the amino acid sequences of NBD1 in MRP1 and several ABC transporters closely related to MRP1. Amino acids sequences of human MRP2, MRP3, MRP4, MRP5, MRP6, CFTR and Pgp were compared to MRP1. The Walker A and B sites, the 13 amino acids MRP subfamily deletion, the ABC signature and the conserved short α helix are indicated by a light grey boxes. The studied phenylalanine residue (or tyrosine in Pgp) is indicated by a dark grey box and a star (*).

was kindly provided by Dr Roger Deeley and Dr Susan Cole (Cancer Research Laboratories and Department of Pharmacology and Toxicology, Queens University, Kingston, Ontario K7L 3N6, Canada).

2.2. Cell culture

The wild-type and mutant overexpressing cells were stably transfected in HEK293 cells grown in DMEM supplemented with 10% fetal bovine serum, 4 mM L-glutamine and 1% of a penicillin/streptomycin/fungizone solution (Gibco BRL, Invitrogen).

2.3. Vector construction and site-directed mutagenesis

A sequence corresponding to a 6-polyhistidine tag was added by site-directed mutagenesis at the 3′ end of the MRP1 gene in the pRC/CMV-MRP1 plasmid in order to purify the protein. Deletion of Phe^{728} in MRP1 was generated using the QuikChange XL™ site-directed mutagenesis kit (Stratagene, La Jolla, CA). The mutagenesis was performed by PCR on the eucaryotic expression vector pRC/CMV-MRP1 with the following mutagenic primer (∗ represents the deleted TTT codon): 5′-CCG AGA AAA CAT CCT ∗ TGG ATG TCA GCT GGA GG-3′. The mutation and the integrity of the rest of the MRP1 gene were verified by DNA sequencing (Eurogentec).

2.4. Transfections of mutant MRPΔF728 expression vector in human embryonic kidney cells (HEK293)

Wild-type pRC/CMV-MRP1 and mutant pRC/CMV-MRPΔF728 expression vectors were transfected into human embryonic kidney cells (HEK 293). Cells were seeded in a 6-wells plate, grown to 80% of the confluence and transfected with the corresponding plasmid using DiC14 amidine, a cationic lipid designed by our team and protamine sulfate, as an activator peptide [22,23]. A stable HEK 293 cell line expressing MRPΔF728 was generated by exposure to geneticin (0.5 μg/ml) for several months.

2.5. Determination of wild-type and mutant levels of expression

The relative levels of wild-type and mutants expression were determined by immunoblot and densitometry analysis. Briefly, 5×10^5 cells were lyzed into Sample Buffer, resolved on SDS–PAGE (7.5%) and electrotransferred to nitrocellulose membrane. Afterwards, membrane was blocked in PBS buffer containing 5% BSA and incubated overnight with the mouse monoclonal primary antibody MRPm6 (dilution 1:4000). The membrane was washed and incubated with an anti-mouse antibody conjugated to horseradish peroxydase (dilution 1:2000). Immunoreactive proteins were visualized by chemiluminescence using ECL Plus Western Blotting detection reagents.

2.6. Fluorescence microscopy

Fluorescence microscopy was performed according to the protocol of Zhang et al. [24]. MRP1 localization was determined using an Axiovert S100 TV (Zeiss) fluorescence microscope (xenon lamp; λ_{ex} and λ_{em} are respectively 540 ± 25 and 605 ± 55 nm for propidium iodide and respectively 480 ± 30 and 560 ± 80 nm for Alexa Fluor 488).

2.7. MTT cells viability test

Briefly, cells were seeded in a 96 wells plate. The day after, various concentrations of drug were added to the cells. After 72 h incubation, drug and medium were removed and 100 μl of the MTT reagent (0.5 mg/ml) was added. After 3 h, the crystals of formazan produced were solubilized by mixing with 100 μl DMSO. Absorbance was determined at 540 nm using an Elisa plate reader (Titertek Multiskan Plus MK II).

2.8. Purification and reconstitution of MRPΔF728

The MRPΔF728-overexpressing cells HEK 293 were lyzed by sonication and the nuclei and unlyzed cells were removed by centrifugation. The plasma membranes were purified on a sucrose gradient, washed twice and pelletted by ultracentrifugation. The membrane proteins were solubilized by an anionic detergent (DDM, *n*-dodecyl-β-D-maltoside) and loaded on a Cobalt Histidine Bind Resin column (Clontech). After the washing steps, the protein bound to the resin thanks to its histidine tag was eluted by a Tris buffer containing 50 mM imidazole. Excess of salt was removed by centrifugation on MicroSpin G-25 columns (Amersham Pharmacia Biotech). Reconstitution of the purified protein into liposomes was performed as described previously [25,35].

2.9. Attenuated total reflection Fourier transform infrared spectroscopy

Attenuated total reflection Fourier transform infrared spectroscopy (ATR-FTIR) spectra were recorded at room temperature on a Bruker IFS55 FTIR spectrophotometer equipped with a liquid nitrogen-cooled mercury-cadmium-telluride (MCT) detector at a nominal resolution of 2 cm^{-1}, and encoded every 1 cm^{-1}. The spectrophotometer was continuously purged with air dried with a FTIR purge gas generator 75–62 Balston (Maidstone, England) at a flow rate of 5.8 l/min. The internal reflection element (ATR) is a germanium plate ($50 \times 20 \times 2$ mm) with an aperture angle of 45°, yielding 25 internal reflections [26],

2.9.1. Sample preparation. The sample contained 20 μg of reconstituted MRP1. For the measurements carried out in the presence of different ligands, the molar protein to ligand ratio is 1/14 for DOX, 1/3 for GSH and 1/6 for ATP. Thin films of oriented multilayers were obtained by slowly evaporating the sample on one side of the ATR plate under a stream of nitrogen [26]. The ATR plate was then sealed in a universal sample holder (Harrick Scientific).

2.9.2. Secondary structure analysis. The sample on the ATR plate was equilibrated with D_2O-satured N_2 for 16 h, at room temperature. 256 scans were averaged for each measurement. The determination of the secondary structure was based on the shape of the Amide I band (1600–1700 cm^{-1}), which is sensitive to the secondary structure [27]. The analysis was performed on the Amide I region of deuterated samples because the H/D exchange allows differentiation of the α-helical secondary structure from the random secondary structure whose absorption band shifts from about 1655 cm^{-1} to about 1642 cm^{-1} [28]. A combination of Fourier self-deconvolution and a least squares iterative curve fitting was applied to narrow and to quantify the area of the different components of Amide I band between 1700 and 1600 cm^{-1} [29]. To avoid the introduction of artifacts due to the self-deconvolution procedure, the fitting was performed on the non-deconvoluted spectrum. The proportion of a particular structure was computed as the sum of the area of all the fitted Lorentzian bands having their maximum in the frequency region where that structure occurs divided by the total area of the Amide I. The frequency limits for each structure were assigned according to theoretical [30] or experimental [31] data: 1662–1645 cm^{-1}, α-helix; 1689–1682 and 1637–1613 cm^{-1}, β-sheet; 1644.5–1637 cm^{-1}, random; 1682–1662.5 cm^{-1}, β-turns.

2.9.3. H/D exchange kinetics. Films containing 20 μg of reconstituted MRP1 were formed on a germanium plate as described above. Nitrogen was saturated with D_2O by bubbling in a series of three vials containing D_2O. Before starting the deuteration, 10 spectra of the sample were recorded to test the stability of the measurements. At zero time, the D_2O-saturated N_2 flux, at a flow rate of 100 ml/min, was connected to the sample. For each kinetic time point, 24 scans were recorded and averaged at a resolution of 2 cm^{-1}. The signal from the atmospheric water was subtracted as described by Goormaghtigh et al. [32]. As previously described [30], deuteration of protein side-chains induces modifications in the Amide I (1700–1600 cm^{-1}) and Amide II (1600–1500 cm^{-1}) regions. Several parameters modulate their contribution including ionization state of the carboxylic amino acids and the fraction of deuterated and undeuterated amino acid side chains for every spectrum of the kinetics. We used homemade software, which can compute the contribution of the amino acid side-chains as a function of the extent of deuteration [33]. The area of Amide II, characteristic of the δ(N–H) vibration, was obtained by integration between 1596 and 1502 cm^{-1}. For each spectrum, the area of Amide II was divided by the corresponding lipidic ν(C=O) area to take into account small but significant variations in the total intensity due to the presence of D_2O which induces swelling of the sample layer at the beginning of the kinetics [28]. This ratio expressed in percentage was plotted versus deuteration time. The value corresponding to 0% of deuteration is defined by the Amide II/lipid ratio before deuteration. The 100% value corresponds to a zero absorption in the Amide II region, observed for full deuteration of the protein.

3. Results

Deletion of phenylalanine 508 in CFTR results in a loss of expression of the membrane protein, which is retained in the endoplasmic reticulum in an inactive form that is rapidly degraded. In MRP1, the position of phenylalanine 728 (F728) is identical to that of F508 in CFTR with respect to the Walker sites (Fig. 1). We expressed the MRPΔF728 mutant and investigated how ΔF728 mutation affects the cell assignment, drug transport activity and structure of MRP1.

3.1. Expression and cellular localization of mutant MRPΔF728 in stably transfected HEK293 cells

Site-directed mutagenesis was performed as described in Section 2. The mutation and the integrity of the rest of the MRPΔF728 gene were verified by DNA sequencing (Eurogentec, results not shown). The eucaryotic expression vector pRC/CMV-MRPΔF728 was used to stably transfect HEK293 cells. After selection of cells resistant to geneticin, we isolated by limiting cell dilution subpopulations of cells expressing MRPΔF728 at a level similar to the one obtained for MRP1 in HEK293 cells. Immunoblotting and densitometry analysis demonstrated that the yield of MRPΔF728 expression in HEK 293 transfected cells is similar to MRP1 (Fig. 2). Indeed the area of the second peak (peak 2) representing the density of the MRPΔF728 band in the immunoblot is about 97% of the area of the first one (peak 1) corresponding to the rate of expression of WT MRP1.

The cellular localization of MRP1 and mutants was determined by fluorescence microscopy on transfected HEK293 cells. Digitonin-permeabilized cells were incubated with a mouse MRP1-specific primary monoclonal antibody MRPm6 which recognizes a linear epitope near the intracellular COOH-terminus of the protein. The secondary mouse antibody Alexa Fluor 488 is visualized by the green fluorescence. Nuclei were coloured in red by propidium iodide. As shown in Fig. 3, cells expressing wild-type (Fig. 3C) and mutants (Fig. 3E) exhibited strong plasma membrane localization, indicating that the ΔF728 mutation did not affect the protein trafficking.

3.2. Cellular localization of mutant MRPΔF728 in transiently transfected HEK293 cells after GSH depletion in the presence or the absence of doxorubicin

BSO is an inhibitor of GSH biosynthesis. In order to describe the cellular targeting of MRPΔF728 in the absence of intracellular GSH, HEK293 cells were incubated during 24 h in 25 μM BSO before transfection. Under these conditions, the intracellular GSH concentration level is reduced by about 90% (data not shown and [34]). Cells were transfected with wild-type and mutant genes-containing expression vectors and incubated again in 25 μM BSO for 48 h. Fluorescence microscopy was performed on transfected and untransfected HEK293 cells as described before. Interestingly, it appears that after GSH depletion, the mutant is no longer routed to the plasma membrane but is retained into the cytoplasm (Fig. 3D). In the same conditions, mutant in the presence of intracellular GSH (Fig. 3E), in the presence of intracellular GSH and doxorubicin (Fig. 3G) and wild-type protein in the absence (Fig. 3B) or in the presence (Fig. 3C) of intracellular GSH were correctly targeted to the plasma membrane. Incubation with doxorubicin after GSH depletion does not restore the routing to the plasma membrane (Fig. 3F).

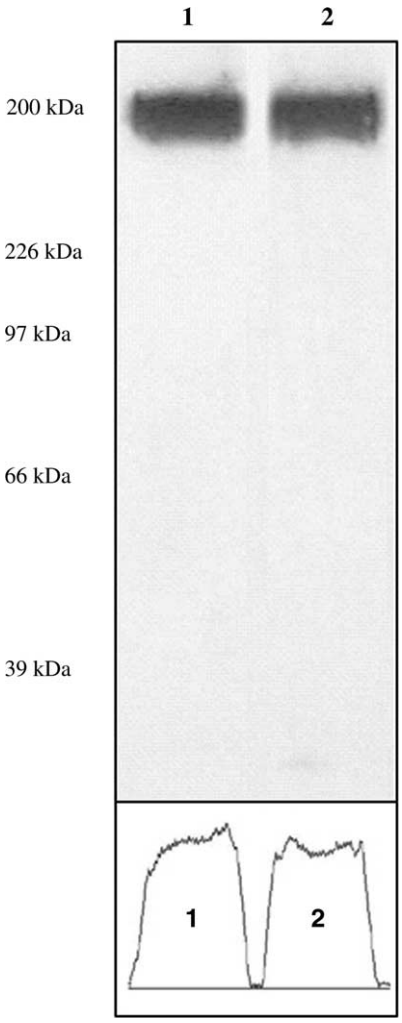

Fig. 2. Western Blot and densitometry analysis on MRP1- and MRFΔF728-overexpressing cells. MRP1 (lane 1) and MRPΔF728 (lane 2) were detected with monoclonal antibody MRPm6. The same quantities of cell lysates were loaded on each lane.

3.3. Antitumoral drug resistance of stably transfected wild-type and mutant MRPΔF728 cells

MRP1 confers resistance to anticancer drugs by rejecting them out of the cells and so reducing their intracellular accumulation. Two antitumoral drugs, an anthracycline (Doxorubicin, DOX) and a *Vinca* alcaloid (Vincristine, VCR) were used to assess the resistance profiles of wild type and mutant ΔF728 overexpressing HEK293 cells. Drug resistance was also determined after BSO-mediated intracellular GSH depletion. Drug resistance of wild-type and mutants overexpressing cells was determined by a cell viability MTT-test following exposure to increasing concentrations of drugs. Results clearly showed a similar drug resistance in cells overexpressing the wild-type or mutant. Indeed the vincristine IC_{50} values for MRP1 or MRPΔF728-overexpressing cells are 18.1 ± 2.1 and 22.6 ± 2.4 nM respectively versus 3.7 ± 0.5 nM for MRP1-not expressing cells. The doxorubicin IC_{50} values were 91 ± 5, 93 ± 9 and 35 ± 5 nM, respectively. Accumulation of Fluo3 (which does not need GSH for its transport) in MRPΔF728 expressing cells treated or not with BSO revealed that in the absence of BSO, cells excreted Fluo3 more efficiently than BSD-treated cells (data not shown).

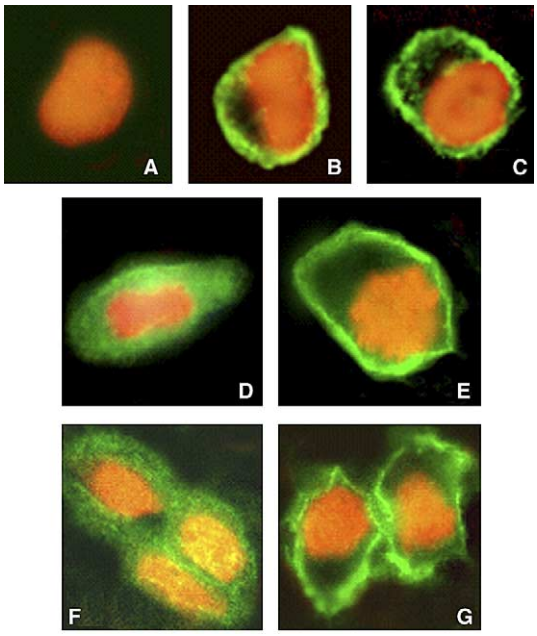

Fig. 3. Fluorescence microscopy of HEK-MRP1 and HEK-MRPΔF728 cells after intracellular GSH depletion and/or doxorubicin incubation. Nuclei are coloured in red by propidium iodide. Wild-type and mutant MRP1 proteins are coloured in green by Alexa fluor 488. (A) Untransfected HEK293 cells; (B) HEK-MRP1 cells after GSH depletion; (C) HEK-MRP1 cells without GSH depletion; (D) HEK-MRPΔF728 cells after GSH depletion; (E) HEK-MRPΔF728 cells without GSH depletion; (F) HEK-MRPΔF728 cells after GSH depletion and incubation with doxorubicin; (G) HEK-MRPΔF728 cells without GSH depletion and after incubation with doxorubicin.

3.4. Comparison of wild-type MRP1 and correctly targeted MRPΔF728 mutant structure

A key point was to know whether MRPΔF728 in the plasma membrane is folded in a "wild-type" configuration. Comparison of the structural characteristics of MRPΔF728 and wild-type MRP1 is a way to address this point. ATR-FTIR spectroscopy has been proven to be an adequate tool to study the structure of a protein in its lipid environment [26–29] even if minimal amounts of protein material are available.

3.4.1. Purification and reconstitution of MRPΔF728 from the plasma membrane. Briefly, solubilized membranes proteins were loaded on a *Talon cobalt histidine bind resin.* The resin was washed twice with 10 volumes column of purification buffer containing successively 1 and 4 mM imidazole. MRPΔF728 was eluted with purification buffer containing high imidazole concentrations (50 mM) without any contaminant protein visible on the gel (Fig. 4, lane 3). This one-step protocol provides us a highly purified MRPΔF728. After concentration and dialysis of the protein sample, it was reconstituted into liposomes of asolectine as described previously [25,35].

3.4.2. MRPΔF728 secondary structure in the lipid bilayer. The secondary structure of MRPΔF728 was determined by Fourier deconvolution and curve-fitting analysis of the amide I band of a deuterated sample as previously described [29]. The proportions of different secondary structures

are similar for MRPΔF728 and MRP1 (41 ± 3% α helix and 29 ± 3% β sheet for MRP1; 40 ± 2% α helix and 28 ± 1% β sheet for MRPΔF728). Both MRPΔF728 and wild-type MRP1 adopt a similar structure when inserted into the plasma membrane.

3.4.3. Kinetics of deuteration of MRPΔF728. At constant pH and temperature, the rate of amide hydrogen exchange by deuterium is related to the stability of the secondary structures and/or to the solvent accessibility of the NH amide groups. Amide hydrogen exchange was followed by monitoring the decrease of the amide *n* absorption peak of MRP1 (maximum at 1544 cm^{-1}) as a function of the time of exposure to D_2O-saturated N_2 flow (Fig. 5). The decreasing area of amide II computed between 100% and 0% (see Section 2) is reported in Fig. 6. 37% of the amide hydrogens of MRPΔF728 remain unexchanged after 2 h of deuteration. One should have in mind that this method is extremely sensitive to minor structural changes and has been used successfully to identify transient structural intermediates involved in ABC transporters [25,35,45]. The fact that the kinetics of deuteration are identical in the limit of the error bars for both proteins demonstrates that the two proteins adopt a similar tertiary structure (Fig. 6).

4. Discussion

A single mutation corresponding to the deletion of phenylalanine 508 in CFTR is responsible for over 70% of the cystic fibrosis (CF). This mutation affects the folding of CFTR which is retained into the endoplasmic reticulum in an immature and inactive form that is rapidly degraded [3–6]. Phenylalanine 508 of CFTR is present in a sequence of 7–9 amino acids which has a propensity to fold as a short α-helix [37,38]. This sequence is located between the Walker A and B sites of NBD1. Studies on short synthetic peptides showed that deletion of F508 from this short α-helix in CFTR destabilizes the entke helix [38,39]. Other studies showed that this destabilization mediates an inhibition of the entire NBD1 folding [40]. Misfolded CFTRAF508 is no longer recognized or accepted by the cellular "quality control" mechanism.

An homologous phenylalanine residue is found at position 728 in MRP1. Oppositely to CFTRΔF508, MRPΔF728 is

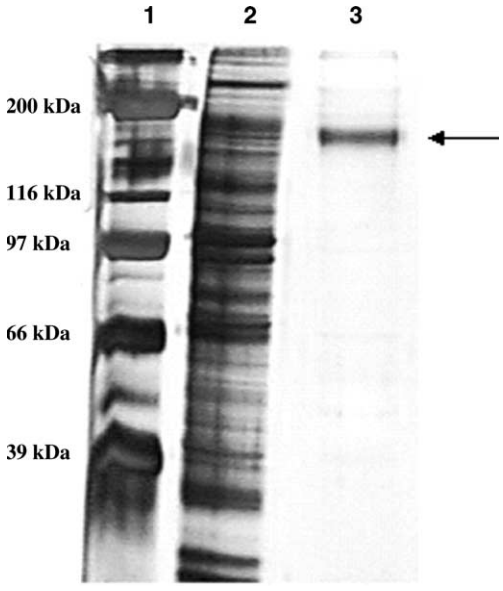

Fig. 4. Purification of MRPΔF728 on cobalt-chelated affinity resin. Lane 1: high range molecular weight markers; lane 2: membrane proteins; lane 3: elution of the mutant with 50 mM imidazole.

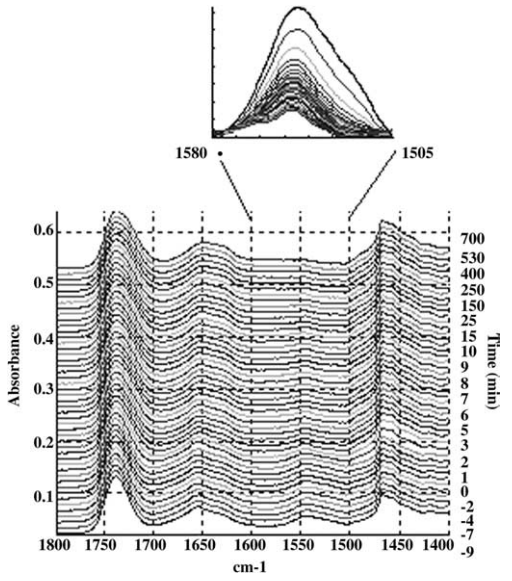

Fig. 5. Infrared spectra in the 1800–1400 cm^{-1} region of MRPΔF728 reconstituted into lipids. Thin films were obtained by slowly evaporating a sample containing 20 μg of MRPΔF728 on an attenuated total reflection element. Spectra were recorded as a function of the time (in minutes) of exposure to D_2O-saturated N_2. Negative times refer to spectra recorded before starting the deuteration procedure. Inset shows the decrease in intensity of the amide II band during the H/D exchange kinetics of MRPΔF728.

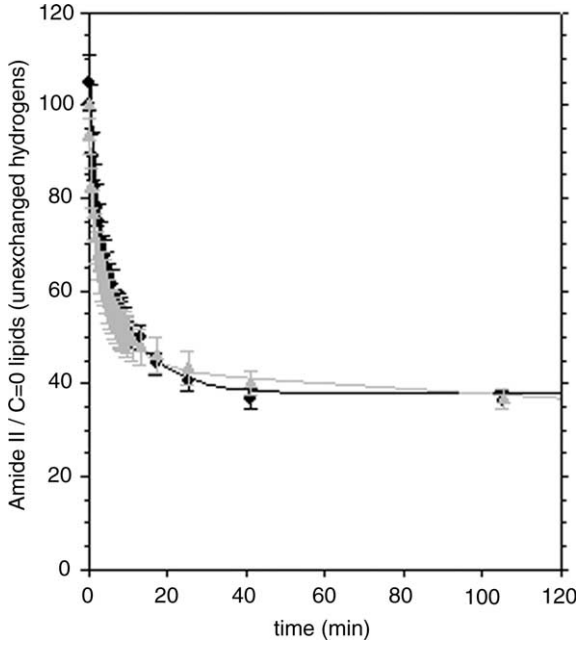

Fig. 6. Evolution of the proportion of unexchanged amide bonds of MRP1 and MRPΔF728 computed between 100% and 0% as a function of the deuteration time. MRP1 (●); MRPΔF728 (▲). The curves are the means of three experiments.

correctly routed to the plasma membrane when expressed in HEK293 cells. Cell multidrug resistance associated to the overexpression of MRP1 is not affected by the ΔF728 mutation. The resistance to two cytotoxic substrates (DOX, VCR) is similar for MRP1 and MRPΔF728 overexpressing cells. Incubation of MRPΔF728 overexpressing cells with doxorubicine does not affect the protein localization. However depletion of intracellular GSH by addition of 25 μM BSO to the culture medium leads to an incorrect protein targeting that is not reverted by addition of the MRP1 substrate doxorubicin. Indeed after intracellular GSH depletion, the protein is not routed to the plasma membrane and is retained into the cytoplasm. Infrared spectroscopy on purified and reconstituted MRPΔF728 mutant demonstrated unambiguously that its secondary structure is similar to the one of MRP1 in the absence of ligands. Recent studies have for the first time demonstrated that GSH binding strongly stabilizes MRP1 and protects it from proteolysis, whereas drug binding renders the protein more accessible. Indeed after 90 min incubation with trypsin, MRP1 in the presence of GSH remains uncleaved [35]. Our hypothesis is that GSH binds to the neo-synthesized protein and stabilizes it in a conformation that is recognized by the "quality control" mechanism and correctly targeted to the plasma membrane. If GSH is absent, the new protein would be retained into the endoplasmic reticulum (ER) or others cytosolic compartments. GSH may act as a specific endogenous chaperone of MRP1, which allows the protein to be correctly folded and targeted. This specificity is plausible since MRP1 presents specific GSH-binding sites and needs GSH to co-transport many drugs. GSH binding sites have recently been identified: one site is located in two cytosolic loops (the loop between the transmembrane helices 5 and 6 and the loop containing the NBD1) and an other one is composed by the transmembrane helices 10, 11, 16 and 17 [44].

Similar rescuing processes have been observed for CFTRΔF508 when cells are grown at lower temperatures or in the presence of glycerol [41,42] that acts as a chemical chaperone [43] and have also been reported for PgpAY490, a Pgp mutant equivalent to MRPΔF728 and CFTRΔF508 [36]. This tyrosine residue Y490 is located in the conserved short helix mentioned above (Fig. 1). As in the case of MRPΔF728 in the absence of GSH and CFTRΔF508, Pgp ΔY490 is not correctly routed to the plasma membrane. It is retained into the cytoplasm in an inactive and defectively processed form. However cells incubation with cyclosporin A, a Pgp-substrate, restores the right processing and targeting of the mutant which becomes as active as the wild-type protein. ATR-FTIR structural characterization performed on Pgp in the presence of another substrate (verapamil) showed a strong stabilization of the protein [45]. This suggests that in contrast to MRP1, a Pgp substrate stabilizes PgpΔYa490 and allows it to be correctly routed. Cyclosporin A acts for PgpΔY490 as a chemical chaperone.

In conclusion, in the absence of intracellular GSH, MRPΔF728 is not correctly routed to the plasma membrane. The presence of GSH strongly stabilizes the mutant and protects it from degradation. This stable conformation allows the protein to be accepted by the cellular "quality control" mechanism, which targets it to the plasma membrane. GSH is finally released and the protein recovers a conformation similar to the wild-type as we verified by IR spectroscopy. These data are in agreement with recent results obtained by our team, which demonstrated that GSH binding strongly stabilizes MRP1 structure and significantly enhances its protection against proteolysis [35]. Our work could also suggest that in cells expressing CFTRΔF508, cytosolic GSH concentration is not sufficient to allow a correct routing of the protein to the plasma membrane.

Acknowledgement: Frédéric Buyse is recipient of financial support from *Fondation Alice et David Van Buuren* and *ARC* (*Action de Recherche Concertée*). Michel Vandenbranden is a Research Associate of the Belgian F.N.R.S. (Fonds National pour la Recherche Scientifique).

References

[1] Riordan, J.R., Rommens, J.M., Kerem, B., Alon, N., Rozmahel, R., Grzelczak, Z., Zielenski, J., Lok, S., Plavsic, N., Chou, J.L., Drumm, M.L., lannuzzi, M.C., Collins, F.C. and Tsui, L.C. (1989) Science 245, 1066–1073.
[2] Sheppard, D.N. and Welsh, MJ. (1999) Physiol. Rev. 79 (suppl. 1), S23–S45.
[3] Cole, S.P.C., Bhardwaj, G., Gerlach, J.H., Mackie, I.E., Grant, C.E., Almquist, K.C., Stewart, A.J., Kurz, E.U., Duncan, A.M.V. and Deeley, R.G. (1992) Science 258, 1650–1654.
[4] Cheng, S.H., Gregory, R.J., Marshall, J., Paul, S., Souza, D.W., White, G.A., O'Riordan, C.R. and Smith, A.E. (1990) Cell 63, 827–834.
[5] Yang, Y., Janich, S., Cohn, J.A. and Wilson, J.E. (1993) Proc. Natl. Acad. Sci. USA 90, 9480–9484.
[6] Kopito, R.R. (1999) Physiol. Rev. 79 (suppl. 1), S167–S173.
[7] Loe, D.W., Almquist, K.C., Deeley, R.G. and Cole, S.P.C. (1996) J. Biol. Chem. 271, 9675–9682.
[8] Breuninger, L.M., Paul, S., Gaughan, K., Miki, T., Chan, A., Aaronson, S.A. and Kruh, G.D. (1995) Cancer Res. 55, 5342–5347.
[9] Lorico, A., Rappa, G., Flavell, R.A. and Sartorelli, A.C. (1996) Cancer Res. 56, 5351–5355.
[10] Muller, E.G.E., de Vries, P.L.M. and Jansen, J. (1996) Hepatology 24, 100–108.
[11] Jedlitschky, G., Leier, L., Buchholz, U., Barnouin, K., Kurz, G. and Keppler, D. (1996) Cancer Res. 56, 988–994.
[12] Loe, D.W., Almquist, K.C., Cole, S.P.C. and Deeley, R.G. (1998) Cancer Res. 58, 5130–5136.
[13] Versantvoort, C.H.M., Broxterman, H.J., Bagrij, T., Scheper, R.J. and Twentyman, P.R. (1995) Br. J. Cancer 72, 82–89.
[14] Bakos, E., Evers, R., Sinko, E., Varadi, A., Borst, P. and Sarkadi, B. (2000) Mol. Pharmacol. 57, 760–768.
[15] Draper, M.P., Martell, R.L. and Levy, S.B. (1997) Eur. J. Biochem. 243, 219–224.
[16] Feller, N., Broxterman, H.J., Wahrer, D.C.R. and Pinedo, H.M. (1995) FEBS Lett. 368, 385–388.
[17] Ueda, K., Taguchi, Y. and Morishima, M. (1997) Sem. Canc. Biol. 8, 151–159.
[18] Loo, T.W. and Clarke, D.M. (1999) J. Biol. Chem. 274, 24759–24765.
[19] Rosenberg, M.F., Mao, Q., Holzenburg, A., Ford, R.C., Deeley, R.G. and Cole, S.P.C. (2001) J. Biol. Chem. 276, 16076–16082.
[20] Hipfner, D.R., Almquist, K.C., Leslie, E.M., Gerlach, J.H., Grant, C.E., Deeley, R.G. and Cole, S.P.C. (1997) J. Biol. Chem. 272, 23623–23630.
[21] Stride, B.D., Valdimarsson, G., Gerlach, J.H., Wilson, G.M., Cole, S.P.C. and Deeley, R.G. (1996) Mol. Pharmacol. 49, 962–971.
[22] El Ouahabi, A., Flamand, V., Ozkan, S., Paulart, F., Vandenbranden, M., Goldman, M. and Ruysschaert, J.M. (2003) Mol. Therapy 7 (1), 81–88.
[23] El Ouahabi, A., Thiry, M., Pector, V., Fuks, R., Ruysschaert, J.M. and Vandenbranden, M. (1997) FEBS Lett. 414, 187–192.
[24] Zhang, D.W., Cole, S.P.C. and Deeley, R.G. (2001) J. Biol. Chem. 276 (16), 13231–13239.

[25] Manciu, L., Chang, X.B., Riordan, J.R. and Ruysschaert, J.M. (2000) Biochemistry 39, 13026–13033.
[26] Goormaghtigh, E., Raussens, V. and Ruysschaert, J.M. (1999) Biochim. Biophys. Acta 1422, 105–185.
[27] Goormaghtigh, E., Cabiaux, V. and Ruysschaert, J.M. (1990) Eur. J. Biochem. 193, 409–420.
[28] Goormaghtigh, E., Cabiaux, V. and Ruysschaert, J.M. (1994) Subcell. Biochem. 23, 363–403.
[29] Goormaghtigh, R., Cabiaux, V. and Ruysschaert, J.M. (1994) Subcell. Biochem. 23, 405–450.
[30] Krimm, S. and Bandekar, J. (1986) Adv. Protein Chem. 38, 181–364.
[31] Byler, D.M. and Susi, H. (1986) Biopolymers 25, 469–487.
[32] Goormaghtigh, E. and Ruysschaert, J.M. (1994) Spectrochim Acta 50, 2137–2144.
[33] Goormaghtigh, E., de Jongh, H.H. and Ruysschaert, J.M. (1996) Appl. Spectrosc. 50, 1519–1527.
[34] Hipfner, D.R., Deeley, R.G. and Cole, S.P.C. (1999) Biochim. Biophys. Acta 1461, 359–376.
[35] Manciu, L., Chang, X.-B., Buyse, F., Hou, Y.-X., Gustot, A., Riordan, J.R. and Ruysschaert, J.M. (2003) J. Biol. Chem. 278, 3347–3356.
[36] Loo, T.W., Bartlett, M.C. and Clarke, D.M. (2002) J. Biol. Chem. 277 (31), 27585–27588.
[37] Bianchet, M.A., Ko, Y.H., Amzel, L.M. and Pedersen, P.L. (1997) J. Bioenerg. Biomembr. 29, 503–524.
[38] Massiah, M.A., Ko, Y.H., Pedersen, P.L. and Mildvan, A.S. (1999) Biochemistry 38, 7453–7461.
[39] Fry, D.C., Byler, D.M., Susi, H., Brown, E.M., Kuby, S.A. and Mildvan, A.S. (1988) Biochemistry 27, 3588–3598.
[40] Qu, B.H. and Thomas, P.J. (1996) J. Biol. Chem. 271 (13), 7261–7264.
[41] Sato, S., Ward, C.L., Krouse, M.E., Wine, J.J. and Kopito, R.R. (1996) J. Biol. Chem. 271, 635–638.
[42] Denning, G.M., Anderson, M.P., Amara, J.F., Marshall, J., Smith, A.E. and Welsh, M.J. (1992) Nature 358, 761–764.
[43] Perlmutter, D.H. (2002) Pediat. Res. 52 (6), 832–836.
[44] Karwatsky, J., Daoud, R., Cai, J., Gros, P. and Georges, E. (2003) Biochemistry 42 (11), 3286–3294.
[45] Sonveaux, N., Shapiro, A.B., Goormaghtigh, E., Ling, V. and Ruysschaert, J.M. (1996) J. Biol. Chem. 271, 24617–24624.
[46] Klein, I., Sarkadi, B. and Varadi, A. (1999) Biochim. Biophys. Acta 1461, 237–262.